

# Grand minima in a buoyancy-driven solar dynamo

M.A.J.H. Ossendrijver

Kiepenheuer-Institut für Sonnenphysik, Schöneckstrasse 6, 79108 Freiburg, Germany (mathieu@kis.uni-freiburg.de)

Received 22 December 1999 / Accepted 3 April 2000

**Abstract.** Numerical simulations of a 2D mean-field model are presented which show that grand minima, typical for the long-term behaviour of solar magnetic activity, can be produced by a dynamo that features an *alpha effect* based on the buoyancy instability of magnetic fluxtubes. The buoyancy-driven alpha effect functions only if the magnetic field strength exceeds a minimal value necessary for instability. It opens the possibility of dynamo action *within* the solar overshoot layer, where a strong magnetic field,  $B \approx 10^5$  G, is thought to be stored. The existence of a magnetic threshold for dynamo action can lead to interruptions of the magnetic cycle, similar to the grand minima of solar activity. Transitions across the instability threshold are triggered by magnetic-flux injections from the convection zone. This is modelled by allowing for a small-scale kinematic alpha effect in the convection zone, and convective downdrafts that penetrate the overshoot layer.

**Key words:** Sun: magnetic fields – Sun: activity – magnetic fields – Magnetohydrodynamics (MHD)

## 1. Introduction

A striking feature in the history of solar activity is the virtual absence of sunspots during the so-called Maunder minimum (1645–1715). Coverage of the sunspot record in this period is estimated to be about two thirds, and the reality of the Maunder minimum is therefore undisputed (Ribes & Nesme-Ribes 1993, Hoyt & Schatten 1996). This and earlier grand minima such as the Spörer minimum (1420–1530) are clearly visible in the records of cosmogenic isotopes, e.g.  $^{14}\text{C}$  and  $^{10}\text{Be}$  (Beer et al. 1998). Timing and duration of the known grand minima are irregular, but the Sun may have experienced grand minima during a third of its history. This is also suggested by observations of magnetic activity of solar-type stars (Baliunas et al. 1995).

Grand minima are the most conspicuous manifestation of solar variability, which is also apparent e.g. in length and amplitude variations of the 11-year sunspot cycle. The spectral and statistical properties of solar variability are still not well-known. Although there is some evidence for various modulations of the solar cycle, among which the 80–90 yr ‘Gleissberg cycle’, it remains doubtful whether they are truly periodic rather

than stochastic. Similarly, the question whether the observations favour an explanation in terms of (quasi-)periodic or chaotic nonlinear behaviour on the one hand, or stochastic processes on the other hand, is as yet unresolved due to the lack of a sufficiently long and accurate dataset.

Various alternative scenarios for grand minima have been suggested. Most of them employ highly idealised nonlinear systems that show quasiperiodic or chaotic intermittent behaviour (e.g. Weiss et al. 1984, Knobloch et al. 1998, Brooke et al. 1998). Küker et al. (1999) considered the backreaction of the magnetic field on differential rotation via quenching of the turbulence in a 2D axisymmetric mean-field calculation. In the present paper, a case is made for a stochastic explanation of grand minima. The motivation stems from several features of the solar dynamo that have been the focus of recent theoretical and computational studies, namely a possible buoyancy-driven alpha effect, convective downdrafts, and small-scale dynamo action in the convection zone.

The magnetic field that emerges in active regions originates as a strong, predominantly toroidal field ( $B \approx 10^5$  G) in the overshoot layer, a thin stably stratified region near the base of the convection zone (Caligari et al. 1995). Helioseismological measurements have demonstrated that radial shear, responsible for the strong toroidal field, is also concentrated near this region (Schou et al. 1998). The generation of the poloidal field from the toroidal field requires an *alpha effect*. Schematically, the alpha effect entails the formation of poloidal loops around an initially toroidal flux element by helical motions (see below for the definition of poloidal and toroidal fields). Given the presence of super-equipartition magnetic fields, a kinematic alpha effect does not function in the overshoot layer, because Lorentz forces inhibit passive advection of the magnetic field by the ambient flow. Hence dynamo models which employ a kinematic alpha effect in the overshoot layer (DeLuca & Gilman 1986, Rüdiger & Brandenburg 1995, Küker et al. 1999) are problematic, unless one would argue that the strong fluxtubes, which are the origin of sunspots, are a secondary phenomenon and play no role in the dynamo. This seems unlikely, since even if the flux were distributed homogeneously in the overshoot region, the magnetic field ought to be dynamically important because its strength would be of the order of the equipartition value (Moreno-Insartis et al. 1992).

A possible solution of this dilemma is offered by a *dynamic* alpha effect based on the magnetic buoyancy instability of toroidal fluxtubes. In a different guise, a similar concept was proposed already by Babcock (1961) and Leighton (1969). The buoyancy-driven alpha effect has also been evoked in the context of the galactic dynamo (Moss et al. 1999) and accretion disks (Arlt & Rüdiger 1999). Schmitt (1987) has shown that non-axisymmetric instabilities of the toroidal field can, under the influence of rotation, give rise to growing magnetostrophic waves that are helical and result in an alpha effect. MHD simulations have confirmed that the magnetic buoyancy instability produces an alpha effect (Brandenburg & Schmitt 1998). Using the thin-fluxtube approximation, Ferriz-Mas et al. (1994) calculated the alpha effect due to a single fluxtube mode, and showed that the mode must be non-axisymmetric and unstable. For typical parameters of the solar overshoot layer, the instability criterium is met for tubes at low latitudes with field strengths larger than about  $10^5$  G. Although the alpha effect of the tube modes increases with increasing instability, in reality fluxtubes cease to contribute significantly to dynamo action if they are highly unstable, since they then escape from the overshoot layer within a very short time.

For field strengths below the instability threshold and somewhat above the equipartition value, fluxtubes in the overshoot layer are stable, and can be perturbed by ambient fluid motions without being shredded. Such random forcing of stable thin fluxtubes does not result in a net alpha effect (Ossendrijver 2000). Thus a solar dynamo based on a magnetic alpha effect is not self-excited: it switches off if a significant number of fluxtubes fail the instability criterium. At that point, the convection zone plays a crucial role, since it continues to generate a magnetic field, which is small-scale, fluctuating, and has a strength of at most the equipartition value (Cattaneo 1999). Some of this flux is carried downward into the overshoot layer by convective downdrafts (Nordlund et al. 1992, Rieutord & Zahn 1995, Tobias et al. 1998), and, where the intensity of the turbulence decreases with depth, by turbulent diamagnetism. Depending on the sign of the field, this leads to accumulation or annihilation of flux in the overshoot layer, thereby enabling occasional transitions from the on-state to the off-state or vice versa.

In the present paper, the scenario of a buoyancy-driven solar dynamo is implemented in a 2D mean-field simulation. Earlier, Schmitt et al. (1996) produced grand minima using a 1D model, in which the flux injections were treated as an additive random source term. The main advantage of a 2D model is that the radial structure is resolved, and that the flux injections can be treated more realistically, namely through the advection term. Of course, mean-field theory cannot replace full MHD calculations, and is at best capable of capturing the main physics of solar dynamo action<sup>1</sup>. The purpose of the calculations is to illustrate that grand minima are an inherent feature of a solar dynamo based on magnetic fluxtubes.

<sup>1</sup> For an introduction to mean-field theory, the first-order smoothing approximation, and a discussion of its limitations, see for instance Krause & Rädler (1980), or Roberts (1995).

## 2. Dynamo model

The induction equation for the mean magnetic field in the *first-order smoothing approximation* is given by

$$\frac{\partial \mathbf{B}_0}{\partial t} = \nabla \times \{ \mathbf{u}_0 \times \mathbf{B}_0 + \alpha \mathbf{B}_0 - \beta \nabla \times \mathbf{B}_0 \}. \quad (1)$$

All mean quantities are defined here as longitudinal averages, so that the mean field,  $\mathbf{B}_0 = (1/2\pi) \int_0^{2\pi} d\phi \mathbf{B}$ , is the axisymmetric component of the actual field. Although the solar magnetic field is highly spatially intermittent, this does not present a formal problem for mean field theory, but merely makes its interpretation more intricate since the translation from actual field to mean field involves a filling factor, i.e.  $B_0 \approx fB$ .

Briefly, the meaning of the various terms in (1) is as follows. The first term describes advection of the mean field by the mean flow. The second term contains the so-called alpha coefficient, which parametrises the effect of helical convection. In the solar dynamo, its main effect is to create a poloidal field from a toroidal field. The third term represents turbulent diffusion, which leads to enhanced transport and decay of the mean field.

The dynamo equation (1) is solved in a spherical shell between  $r = 0.5R$  and  $r = R$ , consisting of a layer with convective overshooting between  $r_1 = 0.6R$  and  $r_2 = 0.7R$ , and a convection zone above it ( $R = 7 \cdot 10^8$  m is the solar radius). Of course, turbulence is not resolved in mean-field theory, and the overshoot layer here merely designates a region of reduced turbulent diffusivity, which for reasons of simplicity is assumed to coincide with the *tachocline*, a layer where the solar rotation rate varies strongly with depth (see below). In reality though, the overshoot layer is probably about 2–3 times thinner than the tachocline (Skaley & Stix 1991). In the overshoot layer, a magnetic filling factor of 0.1 is adopted. If the field strength in the overshoot layer is about  $10^5$  G, this value would suffice to store all the magnetic flux that is seen emerging in active regions (Moreno-Insertis et al. 1992). The filling factor in the convection zone is not well-known. It is set to unity, which is probably an overestimate.

In the simulations, the magnetic field strength is expressed in units of  $B_1 \approx f10^5 \approx 10^4$  G, the threshold value for the buoyancy instability. Time is measured in terms of diffusion times for the convection zone,  $R^2/\beta_0$  (see below).

Two variants of the model are considered, that differ as to how the rapid loss of highly unstable fluxtubes is treated. In model A, an upper threshold is assumed for the magnetic alpha effect. In model B instead, a buoyant upflow with a velocity proportional to the maximum value of  $B_0$  is included.

The mean flow consists of differential rotation, downdrafts, and, for model B, a buoyancy term:

$$\mathbf{u}_0 = \Omega(r, \theta) s \mathbf{e}_\phi + \mathbf{u}_d(r, \theta, t) + \mathbf{u}_b(r, \theta, B_0), \quad (2)$$

where  $s = r \sin \theta$ . For the differential rotation (Fig. 1), the following formula is employed,

$$\begin{aligned} \Omega/\Omega_{\text{eq}} &= 0.9294 - \left[ 1 + \operatorname{erf}\left(\frac{r-r_t}{d}\right) \right] \\ &\times [0.0879 \cos^4 \theta + 0.0534 \cos^2 \theta - 0.0353], \end{aligned} \quad (3)$$

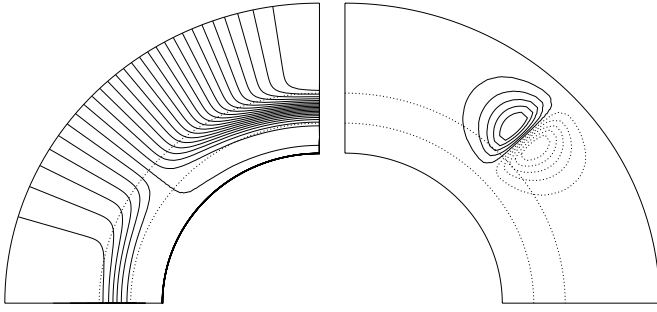


**Fig. 1.** *Left:* internal rotation of the Sun (idealised). Contours are separated by 1% of the maximal rotation rate, which is attained on the surface at the equator. The dotted curves indicate the overshoot layer. *Right:* streamfunction  $\psi$  for a single downdraft. Drawn and dotted contours have anticlockwise and clockwise orientation, respectively. The velocity of the downdraft is everywhere tangent to the contours of  $\psi$ .

which reproduces the main features of the helioseismological results (Schou et al. 1998). The tachocline is somewhat idealised in that all the radial shear is confined to a spherical shell with a thickness of  $0.1R$  (i.e.  $d = 0.05R$ ), centered at  $r_t = 0.65R$ .

The velocity of the downdrafts is derived from a streamfunction,

$$\mathbf{u}_d = \frac{1}{s} \left[ e_r \frac{1}{r} \frac{\partial}{\partial \theta} - e_\theta \frac{\partial}{\partial r} \right] \Psi, \quad (4)$$

where  $\Psi$  consists of  $N$  individual downdrafts, i.e.  $\Psi = \psi_1 + \psi_2 + \dots + \psi_N$ . In all simulations,  $N$  was arbitrarily set to 3. Eq. (4) holds for incompressible flows. Although vertical flows in the Sun are highly compressible in reality, this simple formalism catches the essential feature of the downdrafts, namely localized, rapid downward transport of magnetic flux. As is easily verified, the flow is parallel to the contours of  $\Psi$ , i.e.  $\mathbf{u}_d \perp \nabla \Psi$ . The streamfunction of a single downdraft is modelled as

$$\begin{aligned} \psi = U_d R s & \left[ \operatorname{erf} \left( \frac{\theta - \theta_d}{\vartheta_1} \right) - \operatorname{erf} \left( \frac{\theta - \theta_d}{\vartheta_2} \right) \right] \\ & \times \frac{1}{2} \operatorname{erf} \left( \frac{\theta}{\vartheta_3} \right) \left[ 1 - \operatorname{erf} \left( \frac{\theta - \pi/2}{\vartheta_3} \right) \right] \\ & \times \begin{cases} 0 & (r < r_d) \\ \left[ \frac{4(r - r_d)(R - r)}{(R - r_d)^2} \right]^3 & (r_d \leq r \leq R). \end{cases} \end{aligned} \quad (5)$$

A contour plot of  $\psi(r, \theta)$  is shown in Fig. (1). All downdrafts are assumed to be identical, except for their central colatitude  $\theta_d(t)$ . A factor  $R$  is included for dimensional reasons, and  $r_d = 0.6R$  denotes the lower boundary of a downdraft. The angular scales  $\vartheta_1 = 0.05$  and  $\vartheta_2 = 1$  are chosen such that there is a narrow, rapid downdraft, surrounded by a broad, slow upflow, while the remaining  $\theta$ -dependent factors ( $\vartheta_3 = 0.03$ ) ensure that the flow is purely radial at both equator and pole, as is required for reasons of symmetry. The typical velocity  $U_d$  is expected to be much smaller than the velocity of individual downdrafts because it depends on various filling factors (see below). The correlation time of the downdrafts,  $\tau_d$ , is set to

0.008 diffusion times. Downdrafts are placed simultaneously at randomly chosen latitudes, and are replaced when a correlation time has passed. They are put with equal probability at any latitude, but at least a few degrees away from pole and equator.<sup>2</sup>

The buoyant upflow represents an effective upward advection of the mean field due to the rise of unstable fluxtubes. According to the stability analysis of toroidal fluxtubes, non-axisymmetric modes with azimuthal wavenumbers  $m = 1$  or  $m = 2$  are most likely to become unstable (Ferriz-Mas & Schüssler 1995). Hence, due to the symmetry between upward and downward moving loops of unstable tubes in their linear developmental phase, a net advection of the mean field occurs only during the following nonlinear phase, when downward moving loops become anchored in the overshoot layer while rising loops continue to rise through the convection zone (Caligari et al. 1995). The buoyant upflow is modelled using the same streamfunction as for the downdrafts (4–5), but the constant  $U_d$  is replaced by

$$U = \begin{cases} 0 & (\max B_0 < B_1) \\ U_b \max B_0 / B_1 & (\max B_0 \geq B_1), \end{cases} \quad (6)$$

where  $B_1 \approx f 10^5 \approx 10^4$  G is the instability threshold. One upflow is included. Its location is kept fixed at  $\theta_d = 1.45$ , and its depth,  $r_d = 0.6R$ , is taken to be the same as that of the downdrafts. The linear dependence on the magnetic field is in line with estimates that the velocity of buoyant fluxtubes is comparable to the Alfvén speed,  $u_A = B / \sqrt{\mu_0 \rho}$  (Parker 1975). As in the case of the downdrafts, its typical velocity,  $U_b$ , is expected to be much smaller than the upward velocity of individual rising magnetic loops because it depends on various filling factors (see below).

The total alpha effect consists of a buoyancy-driven term in the overshoot layer, and a small-scale kinematic alpha effect in the convection zone:

$$\alpha = \alpha_0(r, \theta, B_0) + \alpha_1(r, \theta, t, B_0). \quad (7)$$

The magnetic alpha effect is modelled by

$$\begin{aligned} \alpha_0 = \alpha_{0m} \frac{1}{4} & \left[ 1 + \operatorname{erf} \left( \frac{r - r_1}{\delta} \right) \right] \left[ 1 - \operatorname{erf} \left( \frac{r - r_2}{\delta} \right) \right] \\ & \times Q \frac{1}{2} \left[ 1 - \operatorname{erf} \left( \frac{B_0 - B_1}{\delta B} \right) \right] \\ & \times \begin{cases} 0 & (\theta < \theta_0) \\ \sin \left[ \frac{\pi(\theta - \theta_0)}{\pi/2 - \theta_0} \right] & (\theta \geq \theta_0), \end{cases} \end{aligned} \quad (8)$$

where

$$Q = \begin{cases} \frac{1}{2} \left[ 1 + \operatorname{erf} \left( \frac{B_0 - B_2}{\delta B} \right) \right] & (\text{model A}) \\ 1 & (\text{model B}). \end{cases} \quad (9)$$

<sup>2</sup> More accurately, the probability of having a downdraft at colatitude  $\theta$  is roughly proportional to  $\sin \theta$ . The referee is acknowledged for pointing this out. Inclusion of this factor would somewhat enhance the effect of downdrafts near the equator.

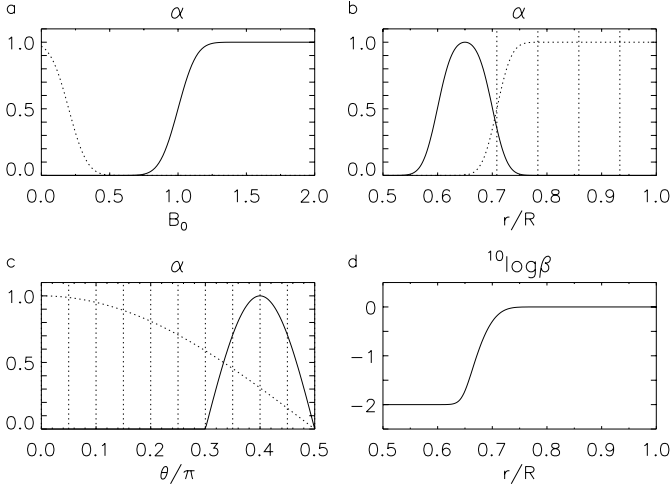


**Fig. 2a–d.** Dynamo coefficients, normalised by the maximum value. **a–c** Alpha in the overshoot layer (drawn curve), and in the convection zone (dotted curve) as a function of **a** the mean magnetic field, **b** radius, and **c** colatitude. **d** Turbulent diffusivity as a function of radius. The dotted vertical lines in **b** and **c** indicate the eddy boundaries in the convection zone.

Here  $\delta = 0.03R$  and  $\theta_0 = 0.3\pi$ . The  $r$ -dependent factor confines alpha to the overshoot layer, and the  $\theta$ -dependent factor confines it to a narrow band centred at the equator. The buoyancy-driven alpha effect functions only at low latitudes, since that is where fluxtubes in the overshoot layer turn out to be appropriately unstable, i.e. where they have growth rates that are neither too small nor too large (Ferriz-Mas & Schüssler 1995). In dimensionless units,  $\delta B$  is set to 0.15. In model A, the factor  $Q$  accounts for an upper threshold,  $B_2 > B_1$ , above which  $\alpha_0$  vanishes, while  $Q$  is unity in model B. The value of  $B_2$  is set to 3.

The kinematic alpha effect in the convection zone has a mean term, and a fluctuating term with zero mean. The former is expected to have roughly a  $\cos \theta$ -dependence, since it is controlled by the Coriolis force. To model the latter, the simple picture of a convection zone consisting of schematic eddies of uniform size is employed. Since the number of eddies on a circle of constant latitude is finite and proportional to  $\sin \theta$ , the averaging over longitude yields rapid residual  $\alpha$ -fluctuations with an amplitude reduced by a factor proportional to  $\sqrt{\sin \theta}$ . In each convective eddy (radial size  $r_c$  set to  $0.075R$ ; latitudinal size  $\theta_c$  set to  $9^\circ$ ; correlation time  $\tau_c$  set to 0.004 diffusion times), an independent random value is assigned to a function  $F$ , satisfying  $\langle F \rangle = 0$  and  $F_{\text{rms}} = 1$ , that is updated when a correlation time has lapsed. Outside the convection zone,  $F = 0$ . The back-reaction of the magnetic field on  $\alpha_1$  through the Lorentz force is modelled by a simple alpha quenching term. It decreases rapidly from unity to zero at a threshold value,  $B_3 = 0.2$ , i.e. about 2000 G in dimensional units, which is of the order of the equipartition field strength:

$$\alpha_1 = \left\{ \alpha_{1m} \cos \theta \left[ 1 + \operatorname{erf} \left( \frac{r - r_2}{\delta} \right) \right] + \delta \alpha_{\text{rms}}^{\text{eq}} \frac{F(r, \theta, t)}{\sqrt{\sin \theta}} \right\}$$

$$\times \frac{1}{2} \left[ 1 - \operatorname{erf} \left( \frac{B_0 - B_3}{\delta B} \right) \right]. \quad (10)$$

Here  $\delta \alpha_{\text{rms}}^{\text{eq}}$  is the rms of the alpha fluctuations at the equator, in the absence of magnetic quenching. Fig. (2) shows the dependence of the alpha coefficients on field strength and spatial coordinates.

In the overshoot layer, the turbulent diffusivity is smaller than in the convection zone because of the convective stability and the presence of strong magnetic fields, both of which reduce turbulence. This behaviour is modelled by setting  $\beta$  to different constant values in the overshoot layer and the convection zone, and allowing  $\beta$  to vary rapidly over a thin layer centered at their boundary according to

$$\beta = \beta_0 \frac{1}{2} \left[ 1 + \epsilon + (1 - \epsilon) \operatorname{erf} \left( \frac{r - r_2}{\delta} \right) \right], \quad (11)$$

where  $\beta_0$  and  $\epsilon \beta_0$  are the turbulent diffusivities in the convection zone and in the overshoot layer, respectively (Fig. 2). In all simulations,  $\epsilon$  was set to 0.01.

The mean field is decomposed into poloidal and toroidal components,

$$\mathbf{B}_0 = \nabla \times P \mathbf{e}_\phi + T \mathbf{e}_\phi, \quad (12)$$

and the  $\alpha\omega$ -approximation is made, i.e. the source term for the toroidal mean field due to the alpha effect is negligible compared to that of the differential rotation. This is motivated by the presence of strong radial shear in the overshoot layer, and strong latitudinal shear in the convection zone. The dynamo equation (1) then reduces to

$$\frac{\partial P}{\partial t} = -\frac{1}{s} (\mathbf{u}_d + \mathbf{u}_b) \cdot \nabla P s + \alpha T + \beta L P \quad (13)$$

$$\begin{aligned} \frac{\partial T}{\partial t} = & -s (\mathbf{u}_d + \mathbf{u}_b) \cdot \nabla \frac{T}{s} + (\mathbf{e}_\phi \times \nabla \Omega) \cdot \nabla P s \\ & + \frac{1}{r} \frac{\partial \beta}{\partial r} \frac{\partial T r}{\partial r} + \beta L T, \end{aligned} \quad (14)$$

where

$$L P = \frac{1}{r} \frac{\partial^2 P r}{\partial r^2} + \frac{1}{r^2} \frac{\partial}{\partial \theta} \frac{1}{\sin \theta} \frac{\partial P \sin \theta}{\partial \theta}. \quad (15)$$

The solutions of (13–14) depend on the following dimensionless parameters:

$$\begin{aligned} C_\omega &= \Omega_{\text{eq}} R^2 / \beta_0, & C_{\alpha 0} &= \alpha_{0m} R / \beta_0, \\ C_d &= U_d R / \beta_0, & C_{\alpha 1} &= \alpha_{1m} R / \beta_0, \\ C_b &= U_b R / \beta_0, & C_{\delta \alpha} &= \delta \alpha_{\text{rms}}^{\text{eq}} R / \beta_0. \end{aligned} \quad (16)$$

In the  $\alpha\omega$ -approximation, solutions are governed by products of (16), the dynamo numbers<sup>3</sup>:

$$C_0 = C_{\alpha 0} C_\omega, \quad C_1 = C_{\alpha 1} C_\omega, \quad C_2 = C_{\delta \alpha} C_\omega. \quad (17)$$

<sup>3</sup> Apart from the ratio  $P/T$ , which is controlled by  $C_{\alpha 0}/C_\omega$ ,  $C_{\alpha 1}/C_\omega$ , and  $C_{\delta \alpha}/C_\omega$ .

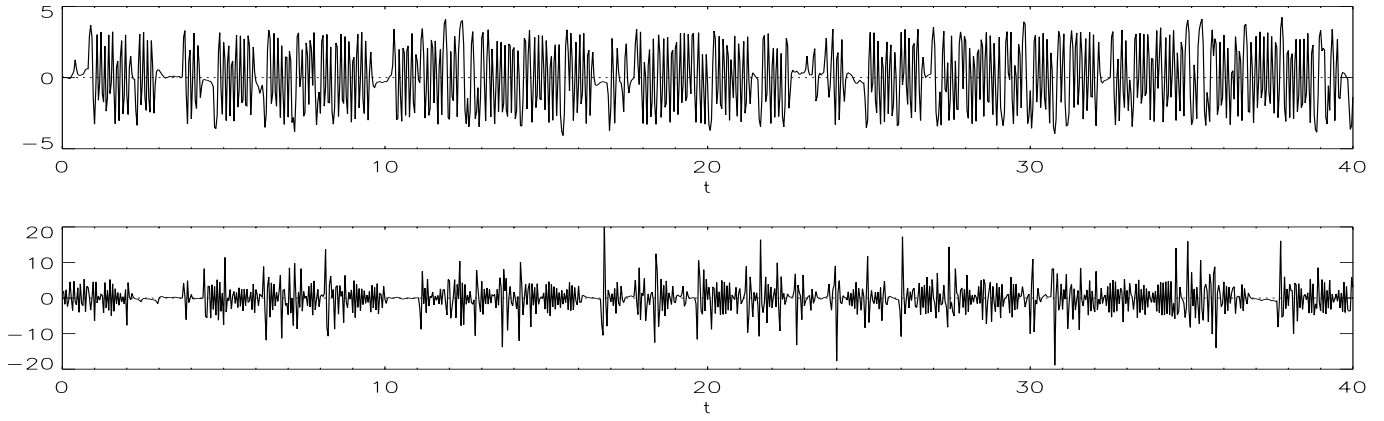


**Fig. 3.** Toroidal field, in units of  $B_1$ , at  $r = 0.625R$  and  $\theta = 0.48\pi$  as a function of time. The time unit is the diffusion time for the convection zone. *Top:* model A ( $C_\omega = 2 \cdot 10^4$ ,  $C_{\alpha 1} = -0.05$ ,  $C_{\alpha 2} = -1$ ,  $C_{\delta\alpha} = 90$ ,  $C_d = -0.06$ , and  $C_b = 0$ ). *Bottom:* model B ( $C_\omega = 2 \cdot 10^4$ ,  $C_{\alpha 1} = -0.05$ ,  $C_{\alpha 2} = -1$ ,  $C_{\delta\alpha} = 100$ ,  $C_d = -0.1$ , and  $C_b = 0.014$ ).

When the alpha effect in the overshoot layer is active, non-decaying solutions are obtained if  $|C_0|$  exceeds a critical value. When the alpha effect in the overshoot layer is inactive, the magnetic field is produced entirely within the convection zone. Obviously, this field should be non-decaying, so that at some later time the dynamo may switch from the off-state to the on-state. Hence  $|C_1|$  or  $|C_2|$  must also exceed a critical value.

As far as known, the predominant parity of the solar cycle has been antisymmetric with respect to the equator. For somewhat supercritical values of  $C_0$ , the fastest-growing mode of the model is an oscillatory antisymmetric mode. However, symmetric modes appear to have only slightly smaller growth rates than antisymmetric modes, as has been observed more often for mean-field dynamos in spherical shells (Moss et al. 1992). The resulting interference of symmetric modes with the dominant antisymmetric was found to produce unrealistically asymmetric butterfly diagrams in simulations performed on two hemispheres. In order to avoid this problem antisymmetry with respect to the equator is imposed, and this allows the integration to be confined to one hemisphere. Clearly, this choice has the disadvantage that several interesting features related to asymmetry, such as the possibility to have grand minima on one hemisphere only, can not be investigated. The complete set of boundary conditions is as follows:

$$\begin{aligned}
 r/R = 0.5 & \quad P = \frac{\partial T r}{\partial r} = 0 \text{ (no field penetration)} \\
 r/R = 1 & \quad \text{match } \mathbf{B}_0 \text{ to potential field} \\
 \theta = 0 & \quad P = T = 0 \\
 \theta = \pi/2 & \quad \frac{\partial P \sin \theta}{\partial \theta} = T = 0 \text{ (antisymmetry)}.
 \end{aligned} \tag{18}$$

At the outer boundary, the magnetic field is matched to a potential field, which satisfies  $\nabla \times \mathbf{B}_0 = 0$ , i.e.  $LP = 0$  and  $T = 0$ .

The model yields butterfly diagrams with equatorward migration only for negative  $C_0$ , which requires a net negative alpha effect on the northern hemisphere. By contrast, the thin-fluxtube

analysis of Ferriz-Mas et al. (1994) and the MHD simulations of Brandenburg & Schmitt (1998) predict a mostly positive alpha on the northern hemisphere. Other MHD simulations suggest a negative sign (Brandenburg et al. 1990). At this point, the sign of the net alpha effect in the solar convection zone has not been definitely established. In principle, equatorward migration can occur also for positive alpha on the northern hemisphere, namely in combination with a meridional flow that is equatorward at the base of the convection zone (Choudhuri et al. 1995). Since this is beyond the goal of the present paper, alpha is assumed to be negative on the northern hemisphere.

A familiar problem of solar dynamo models in thin shells is the presence of more than one polarity belt on each hemisphere, whereas the solar butterfly diagram suggests there should be only one. This problem is only partially alleviated here by confining the magnetic alpha effect to a narrow band at the equator. A more promising way to avoid overlapping polarity belts would be the introduction of an anisotropic diffusivity in the overshoot layer, an issue that will be addressed in a subsequent paper. At present though, no detailed agreement of the butterfly diagram with solar observations is envisaged.

### 3. Numerical solutions

The numerical integration is carried out using an alternating-direction implicit 2D code developed by D. Schmitt and T. Prautzsch of Göttingen. The grid size is set to 61 points in the radial direction, and 51 in the latitudinal direction. The top figures of (3) and (4) show a run for model A, while the bottom figures show model B. In both cases, the magnetic cycle is interrupted irregularly by intervals of low activity, reminiscent of grand minima. The results of both models are similar, the main difference being the size of the magnetic excursions. In model B these are larger, because they are punished less severely, namely through a change of the buoyant upflow, instead of through a more drastic cut-off of the alpha effect. Fig. (6) shows two snapshots of the magnetic field taken from the same simulation of model B that is shown in Fig. (4).

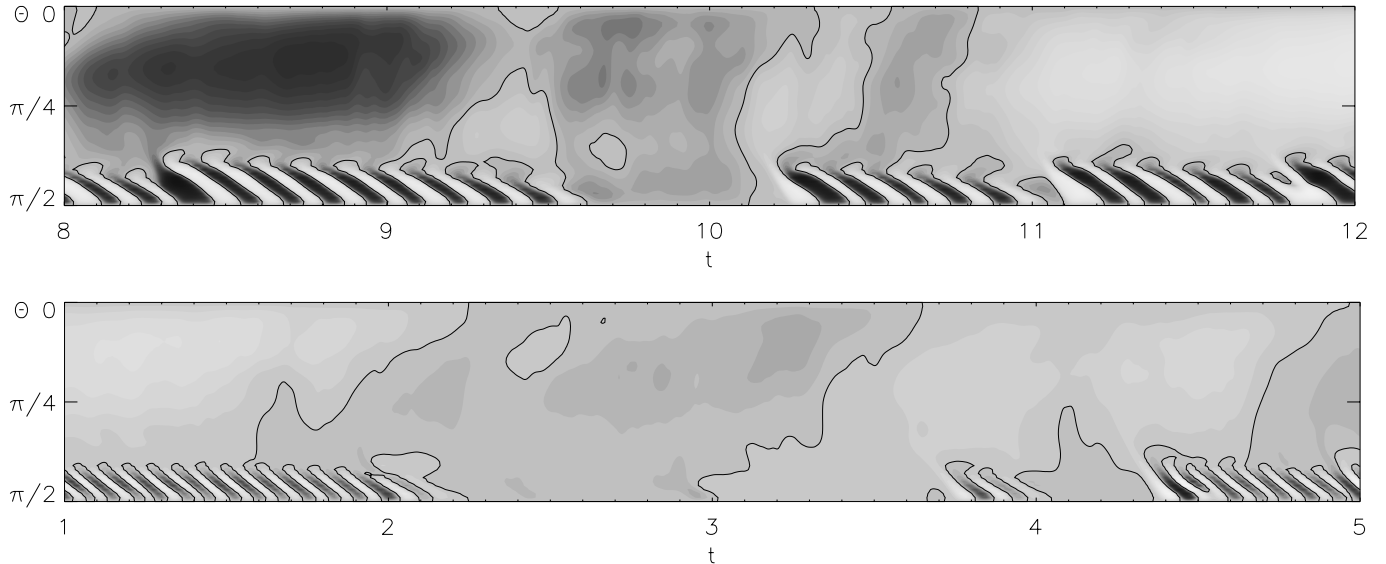


**Fig. 4.** Butterfly diagram of the toroidal field at  $r = 0.625R$  for subintervals of the runs shown in Fig. (3). Light and dark grey indicate positive and negative polarity, respectively; the drawn curve is the zero level. *Top:* model A. *Bottom:* model B.

In order to clarify the effects of the alpha fluctuations and the downflows, Fig. (5) shows a butterfly diagram for the overshoot layer obtained from a short run of model A, that consists of three different phases. During the first phase, the convection zone dynamo and the downdrafts are inactive, and the result is a cyclic magnetic field of constant amplitude. As the convection zone dynamo is switched on in the second phase, the magnetic field in the overshoot layer is perturbed only mildly, because turbulent diffusion rather effectively smears out the small-scale magnetic field while it is transported downward. Alpha fluctuations alone can bring about the transitions only if  $C_0$  is very close to criticality (Ossendrijver et al. 1996). Although this is possible in principle, there is little reason why  $C_0$  would happen to fulfill such a condition in the Sun. In the third phase, the convective downdrafts are switched on, and the variability increases because more flux penetrates the overshoot layer. The enhanced transport due to downdrafts may be interpreted as an increase of the turbulent diffusivity, which makes the dynamo effectively less supercritical, thus facilitating transitions in spite of the supercritical dynamo number. Clearly, the dynamo in the overshoot layer can be turned on again only if the downdrafts carry flux. If the convection zone dynamo is artificially turned off during an off phase, the downdrafts do not carry flux, and the overshoot dynamo never recovers.

For a quantitative comparison of the simulations with solar parameters, the dimensionless parameters (16) are translated into dimensional numbers. From Fig. (4) the dimensionless dynamo period  $P\beta_0/R^2$  is estimated to be about 0.13 in model A, and about 0.08 in model B. Since  $P$  is about 22 years, it follows that  $\beta_0 \approx 9 \cdot 10^7 \text{ m}^2 \text{ s}^{-1}$  (A) and  $6 \cdot 10^7 \text{ m}^2 \text{ s}^{-1}$  (B), close to the typical solar estimate,  $10^8 \text{ m}^2 \text{ s}^{-1}$ .

With these numbers for  $\beta_0$ , one finds that  $C_\omega = 20000$  corresponds to  $\Omega_{\text{eq}} \approx 4 \cdot 10^{-6} \text{ s}^{-1}$  (A) and  $2 \cdot 10^{-6} \text{ s}^{-1}$  (B) respectively, close to the solar value,  $2.8 \cdot 10^{-6} \text{ s}^{-1}$ . From  $C_\alpha =$

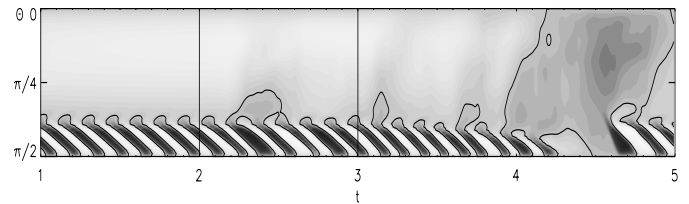


**Fig. 5.** Butterfly diagram of the toroidal field at  $r = 0.625R$  for model A. Parameters are the same as in Fig. (3). The alpha fluctuations are switched on at  $t = 2$ , and the downdrafts at  $t = 3$ .

$-0.05$  it follows that the magnitude of the magnetic alpha effect is  $\alpha_{0m} \approx -7 \cdot 10^{-3} \text{ m s}^{-1}$  (A) and  $-4 \cdot 10^{-3} \text{ m s}^{-1}$  (B). The absolute value of  $\alpha_{0m}$ , though not its sign, is in rough agreement with the results of Ferriz-Mas et al. (1994), who derive values of at most a few  $\text{cm s}^{-1}$ .

The value of  $C_{\alpha\alpha}$  was set to 90 (A) and 100 (B) respectively, and it was verified that these numbers exceed the critical value of  $C_{\alpha\alpha}$  for the off phase. The corresponding rms strength of the alpha fluctuations is  $\delta\alpha_{\text{rms}}^{\text{eq}} \approx 12 \text{ m s}^{-1}$  (A), and  $8 \text{ m s}^{-1}$  (B). Since alpha is an average over longitude, the underlying alpha fluctuations of individual eddies are larger by about a factor  $\sqrt{N_c}$ , where  $N_c$  is the number of eddies on a circle of constant latitude. If one identifies the eddies with giant cells,  $N_c$  is of the order 10. Thus alpha in individual eddies is of the same order as the rms convective velocity near the base of the convection zone (typically  $50 \text{ m s}^{-1}$ ), which constitutes an upper bound for the kinematic alpha effect. The correlation time of the alpha fluctuations,  $\tau_c = 4 \cdot 10^{-4}$ , corresponds to 25 days in model A and 40 days in model B, comparable to typical values associated with giant-cell convection in the lower part of the convection zone.

In order to assess the velocity of the downdrafts and the upflow, consider their maximal radial speed. For a downdraft

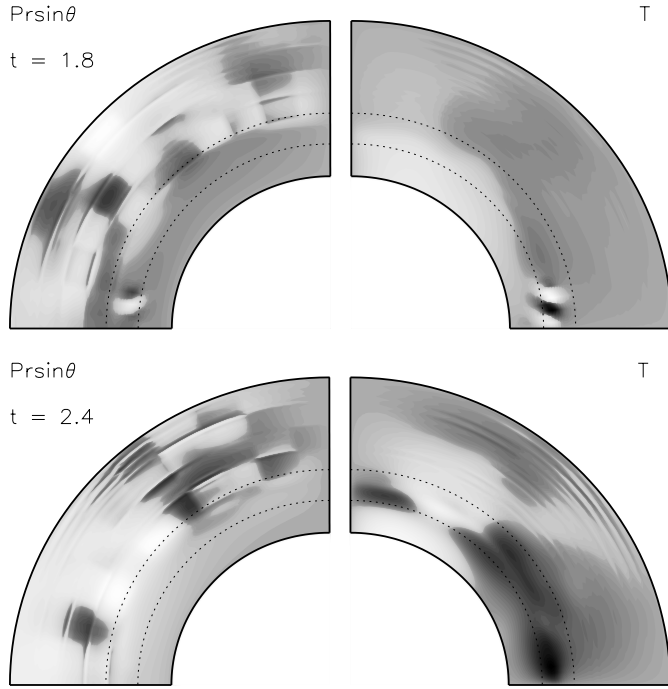


**Fig. 6.** Snapshots of  $Pr \sin \theta$  and  $T$  for model B. The contours of  $Pr \sin \theta$  correspond to fieldlines of the poloidal magnetic field. Light and dark grey indicate positive and negative polarity, respectively. *Top*: on phase. The poloidal field is produced within the overshoot layer. The toroidal field in the overshoot layer is organised in strong low-latitude belts of alternating polarity. *Bottom*: off phase. The poloidal field is created only in the convection zone. As during an on phase, the toroidal field is concentrated in the overshoot layer, but it extends to higher latitudes.

that is located at some distance from pole and equator, so that the second line in (5) is approximately unity, one obtains from (4) and (5) by setting  $r = (R + r_d)/2$  and  $\theta = \theta_d$

$$U_{\max,d} = \frac{U_d}{1 + r_d/R} \frac{2}{\sqrt{\pi}} \left( \frac{1}{\vartheta_1} - \frac{1}{\vartheta_2} \right) \approx 13 U_d. \quad (19)$$

Both  $C_d = -0.06$  (A) and  $C_d = -0.1$  (B) yield  $U_{\max,d} \approx -0.10 \text{ m s}^{-1}$ . The actual velocity of *individual* downdrafts near the base of the convection zone is probably a few times the typical convective velocity, i.e. about  $-100 \text{ m s}^{-1}$ . The much smaller downdraft velocity in the mean-field simulations can be explained as follows. First, the downdrafts are surrounded by a slow upward return flow, which, due to the averaging over longitude, partially cancels the downflow. Secondly, the downdrafts are likely to have a small filling factor (Zahn 1991), and this further reduces the mean flow. Thirdly, the magnetic field in the overshoot layer, if organised in strong fluxtubes, may have a filling factor as low as 10%. Spatial intermittency dilutes the interaction of the downflows with the magnetic field, and this also translates into a smaller mean flow. If each of the factors is about 0.1, which seems reasonable,  $U_{\max,d}$  has the right order of magnitude. The correlation time of the downdrafts,  $\tau_d = 8 \cdot 10^{-4}$ , corresponds to 50 days in model A, and 80 days in model B.

For the buoyant upflow in model B ( $C_b = 0.014$ ) one finds  $U_{\max,b} \approx 0.016 (\max B_0/B_1) \text{ m s}^{-1}$ . From thin-fluxtube calculations it is estimated that the radial velocity of the summit of a rising tube in the convection zone is typically a few times  $100 \text{ m s}^{-1}$  (Caligari et al. 1995). These numbers may be reconciled in a similar fashion as was done for the downflows. First, only a fraction of an unstable tube takes part in the buoyant rise, while other sections remain virtually anchored in the overshoot layer. Secondly, only a small fraction of the fluxtubes in the overshoot layer are likely to be unstable and form rising loops. Thirdly, the filling factor of fluxtubes needs to be taken into account. A rough estimate then suggests that the upflow in the simulations has the right order of magnitude if about 0.1–1% of the fluxtubes in the overshoot layer form rising loops, and this seems a reasonable number.

#### 4. Discussion

The purpose of the present 2D simulations has been to explore the possibility of a solar dynamo based on a magnetic alpha effect, and in particular whether such a dynamo can explain the grand minima of solar activity. The main features of the model are as follows. In the overshoot layer, a magnetic alpha effect operates if the field strength of the magnetic fluxtubes exceeds a threshold for buoyancy instability. Hence the strong fluxtubes that are the source of sunspots are treated not as a secondary phenomenon, but as a crucial ingredient of the solar dynamo. In that sense, the fluxtube scenario (Schüssler 1993) is related to the models of Babcock (1961), Leighton (1969), and Durney (1997 and references therein), which differ mainly in that they attribute the generation of the poloidal magnetic field to eruptions at the solar surface rather than in the interior.

In the convection zone, small-scale dynamo action generates a magnetic field with a strength comparable to the equipartition value. Mainly for reasons of consistency, the mean value of the kinetic alpha effect is assumed to be non-vanishing and proportional to  $\cos \theta$ . In fact, the alpha fluctuations dominate, and the mean term in the convection zone can be set to zero, with no fundamental changes in the result. This shows that even a fully incoherent  $\alpha\omega$ -dynamo in the convection zone would be capable of maintaining sufficient magnetic energy during grand minima. Incoherent dynamo action is known to be capable of producing large-scale magnetic fields *by itself* in accretion disks (Vishniac & Brandenburg 1997). In the present calculation however, its function is to trigger the buoyancy-driven dynamo.

Together with the differential rotation, the alpha terms result in  $\alpha\omega$ -type dynamo action both in the overshoot layer and in the convection zone. The former is responsible for a strong, cyclic field, while the latter generates a weak irregular field. Downdrafts provide enhanced transport of flux between the overshoot layer and the convection zone, thus enabling stochastic transitions between on- and off-states, also for supercritical dynamo numbers.

Weak points of the model are the presence of overlapping opposite-polarity bands in the butterfly diagram, and the anti-symmetry that was imposed on the solutions. Although in such a

schematic model not all details of the butterfly diagram should be expected to agree with solar observations, one may speculate that these two aspects can be resolved by allowing for anisotropic diffusivity in the overshoot layer. Enhanced diffusion in the lateral direction tends to increase the wavelength for that coordinate, and can lead to a more pronounced dominance of the dipolar mode. This would remove the necessity of reducing the integration to a single hemisphere, and enable an investigation of north-south asymmetries in the butterfly diagram. A further possibly problematic feature concerns the strength of the alpha fluctuations in the convection zone. They are large compared to the constant term, though still smaller than the typical convective velocity, which represents an upper bound. While it is well known from box simulations of magnetoconvection that the kinematic alpha coefficient is an extremely noisy quantity (Brandenburg et al. 1990), it is difficult to assess how realistic the level of fluctuations in the model is, since all quantities are averages over longitude.

The other free parameters of the model are more or less consistent with solar estimates. In principle, various properties such as the typical duration of grand minima and how often they occur can be adjusted by changing the dynamo numbers, the speed of the downdrafts and other parameters. However, that would be beyond the goal of these mean-field calculations, which is mainly illustrative.

The intermittency of solar activity is explained here as a stochastic phenomenon, since transitions between on and off-states are the cumulative effect of random flux injections from the convection zone. Intermittency is also a well-known feature of nonlinear dynamical systems (Platt et al. 1993), and it is frequently invoked as a non-stochastic explanation for grand minima (e.g. Knobloch et al. 1998, Tworkowski et al. 1998, Brooke et al. 1998, Tavakol & Covas 1999). It is unclear whether the highly supercritical dynamo numbers, required for nonlinear intermittency, can be justified for the Sun, although the possibility cannot be excluded. Here the case is made that stochastic effects combined with a magnetic alpha effect yield a promising alternative explanation, which requires only moderately supercritical dynamo numbers. Nonlinear effects are invoked only in order to prevent unlimited growth of the magnetic field.

According to the model, the dynamo mechanism during an on phase is qualitatively different from that during an off phase. Such a difference is supported by the virtual absence of sunspots during the Maunder minimum. In spite of this, measurements of the cosmogenic isotope  $^{10}\text{Be}$  in arctic ice cores suggest that the solar cycle may have continued at a reduced level (Beer et al. 1998). A recent more thorough statistical analysis has shown that the  $^{10}\text{Be}$  data are not easy to interpret, especially during grand minima (Fligge et al. 1999). Further confirmation is needed in order to establish beyond doubt the possible continuation of the 11-year solar cycle during grand minima. Although model B does occasionally exhibit intervals of small-amplitude cycles, they are not likely to be a typical feature of a buoyancy-driven dynamo.

An alternative scenario for the solar dynamo is the *interface model*, which features a non-magnetic, kinematic alpha

effect in the convection zone, spatially separated from a shear layer (Parker 1993, Tobias 1996, Charbonneau & MacGregor 1997, Ossendrijver & Hoyng 1997). The kinematic alpha effect functions only for a weak magnetic field, and would therefore more easily account for a continuation of cyclic dynamo action during grand minima. Since it is expected to have roughly a  $\cos\theta$ -dependence, and because solar differential rotation is also strongest near the poles, the result would be dynamo action concentrated at high latitudes, which is not observed. Nevertheless, this need not be in conflict with the observed latitude distribution of sunspots, because at high latitudes, the growth rates of unstable fluxtubes tend to become very long, so that in practice these fluxtubes may not erupt and form sunspots at all (Caligari et al. 1995). However, strong magnetic fields pose a problem for the interface model. Even if the spatial separation between the overshoot layer and the alpha effect does relax the stifling back-reaction of the magnetic field on alpha, it renders the dynamo rather inefficient, because *continuous* exchange of flux between the overshoot layer and the convection zone is required. If the classical alpha effect is quenched significantly for field strengths much weaker than the equipartition value (Vainshtein & Cattaneo 1992), the quenching problem becomes even more severe, and super-equipartition magnetic fields in the overshoot layer would seem very hard to explain (Charbonneau & MacGregor 1996). In this respect, the main advantage of the fluxtube scenario is that strong magnetic fields do not counteract the alpha effect, but actually produce it.

*Acknowledgements.* The author would like to thank M. Schüssler and D. Schmitt for useful discussions.

## References

- Arlt R., Rüdiger G. 1999, A&A 349, 334  
 Babcock H.W. 1961, ApJ 133, 572  
 Baliunas S.L., Donahue R.A., Soon W.H. et al. 1995, ApJ 438, 269  
 Beer J., Tobias S., Weiss N. 1998, Sol. Phys. 181, 237  
 Brandenburg A., Schmitt D. 1998, A&A 338, L55  
 Brandenburg A., Nordlund A., Pulkkinen P., Stein R.F., Tuominen I. 1990, A&A 232, 277  
 Brooke J.M., Pelt J., Tavakol R., Tworkowski, A. 1998, A&A 332, 339  
 Caligari P., Moreno-Insertis F., Schüssler M. 1995, ApJ 441, 886  
 Cattaneo F. 1999, in: *Motions in the Solar Atmosphere*, A. Hanslmeier, M. Messerotti (eds.), Kluwer, Astrophysics and Space Science Library, Vol. 239, p. 119  
 Charbonneau P., MacGregor K.B. 1996, ApJ 473, L59  
 Charbonneau P., MacGregor K.B. 1997, ApJ 486, 502  
 Choudhuri A.R., Schüssler M., Dikpati M. 1995, A&A 303, L29  
 DeLuca E.E., Gilman P.A. 1986, Geoph. Astroph. Fluid Dyn. 37, 85  
 Durney B.R. 1997, ApJ 486, 1065  
 Ferriz-Mas A., Schüssler M. 1995, Geoph. Astroph. Fluid Dyn. 81, 233  
 Ferriz-Mas A., Schmitt D., Schüssler M. 1994, A&A 289, 949  
 Fligge M., Solanki S.K., Beer J. 1999, A&A 346, 313  
 Hoyt D.V., Schatten K.H. 1996, Sol. Phys. 165, 181  
 Knobloch E., Tobias S.M., Weiss N.O. 1998, MNRAS 297, 1123  
 Krause F., Rädler K.-H. 1980, *Mean-Field Magnetohydrodynamics and Dynamo Theory*, Pergamon  
 Küker M., Arlt, R., Rüdiger G. 1999, A&A 343, 977

- Leighton R.B. 1969, ApJ 156, 1
- Moreno-Inertis F., Schüssler M., Ferriz-Mas A. 1992, A&A 264, 686
- Moss D., Brandenburg A., Tavakol R., Tuominen I. 1992, A&A 265, 843
- Moss D., Shukurov A., Sokoloff D. 1999, A&A 343, 120
- Nordlund Å., Brandenburg A., Jennings R.L. et al. 1992, ApJ 392, 647
- Ossendrijver M.A.J.H. 2000, A&A, to appear
- Ossendrijver M.A.J.H., Hoyng P. 1997, A&A 324, 329
- Ossendrijver M.A.J.H., Hoyng P., Schmitt D. 1996, A&A 313, 938
- Parker E.N. 1975, ApJ 198, 205
- Parker E.N. 1993, ApJ 408, 707
- Platt N., Spiegel E.A., Tresser C. 1993, Phys. Rev. Letters 70, 279
- Ribes J.C., Nesme-Ribes E. 1993, A&A 276, 549
- Rieutord M., Zahn J.P. 1995, A&A 296, 127
- Roberts P.H. 1995, in: *Lectures on Solar and Planetary Dynamos*, M.R.E. Proctor, A.D. Gilbert (eds.), Cambridge University Press, p. 1
- Rüdiger G., Brandenburg A. 1995, A&A 296, 557
- Schmitt D. 1987, A&A 174, 281
- Schmitt D., Schüssler M., Ferriz-Mas A. 1996, A&A 311, L1
- Schou J., Antia H.M., Basu S. et al. 1998, ApJ 505, 390
- Schüssler M. 1993, in: *The Cosmic Dynamo*, IAU Symposium 157, F. Krause, K.-H. Rädler, G. Rüdiger (eds.), Kluwer, p. 27
- Skaley D., Stix M. 1991, A&A 241, 227
- Tavakol R., Covas E. 1999, in: *Stellar Dynamos: Nonlinearity and Chaotic Flows*, ASP Conference Series 178, M. Núñez, A. Ferriz-Mas (eds.), San Francisco
- Tobias S.M. 1996, A&A 307, L21
- Tobias S.M., Brummel N. H., Clune Th.L., Toomre J. 1998, ApJ 502, L177
- Tworkowski A., Tavakol R., Brandenburg A. et al. 1998, MNRAS 296, 287
- Vainshtein S.I., Cattaneo F. 1992, ApJ 393, 165
- Vishniac E.T., Brandenburg A. 1997, ApJ 475, 263
- Weiss N.O., Cattaneo F., Jones C.A. 1984, Geoph. Astroph. Fluid Dyn. 30, 305
- Zahn J.-P. 1991, A&A 252, 179